

1 Introduction

Recently FFAG type machines have been proposed for the acceleration of muons because of the (in principle) very large transverse acceptance. The combination of the short muon lifetime and the requirement for large particle transmission dictates that extreme rates of acceleration be used; on the order of 1.5 MeV/metre over several kilometres. Hence, the speed and momentum of reference particles changes appreciably from cell to cell of the magnetic lattice. Consequently, cell traversal time, path length and optical properties change with the reference energy from cell to cell.

1.1 Acceleration by RF cavities

Of course, the cell traversal times must be synchronized with the waveforms in the RF cavities responsible for acceleration. In a linear accelerator composed of independently phased cavities, through which particles travel only once, synchronization would not be a problem. However in a circular machine, particles must make repeated passages through the same cavities; and on every revolution of the machine the frequency and phasing of each cavity must be readjusted.

1.1.1 Proton synchrotron

In a conventional synchrotron-type machine, with acceleration distributed over many thousands of turns, these adjustments are (usually) adiabatic and can be easily accommodated by the cavity filling times. Under these circumstances, the RF and bunch trains appear periodic and it is customary to introduce the notions of harmonic number, synchronous phase and 'RF bucket' of stable oscillations. [Note, if part of the ring is unfilled then it is possible to operate with non-integer harmonic number and have the RF system contract or expand the RF train in the beam gap; this is done at the BNL AGS and CERN SPS for special applications.]

1.1.2 Muon FFAG

In the proposed muon accelerators, by contrast, acceleration is completed in a few turns (< 10) and the RF adjustments needed are impractically large and fast. Even if this adjustment were possible, the fast variation of cell traversal time and path length means that the notions of synchronous phase and RF bucket cannot be applied to the particle trajectories. The usual ideas of synchrotron longitudinal dynamics are not relevant to this type of machine; **even if one could "get the phases right" the longitudinal dynamics would not be simple.**

1.1.3 Selectivity

The FFAG is a very capable transport channel with an enormous acceptance: almost any beam we put into it will be spat out a few turns later; but not necessarily at the correct energy. This lack of discrimination implies that we have to select particles of the correct energy based on their arrival time, which in turn means that one has to keep the beam bunched.

1.2 High-Q cavities

Let us understand the RF power requirements. There are designs available for 200 MHz normal conducting (NC) and 400 MHz superconducting cavities (SC) to be used in CERN LHC that provide a starting point for extrapolation. Let us imagine 60 MW of wall-plug power is available and that it can be converted to RF power at the accelerating gap with 50% efficiency. If there are 300 NC cavities, then allowed power consumption is 100 kW per cavity. Each cavity has 1.4 MV gap voltage and so the shunt resistance has to be 10 Mohm or more. The ratio of resistance to quality factor (R/Q) depends on cavity geometry, and approaches 200 for the CERN cavities. Hence, in this scenario (30 MW & NC cavities) the quality factor must be at least 5×10^4 .

The cavity output faithfully follows its input for variations comparable with (or slower than) the cavity filling time. The filling time is equal to quality factor multiplied by RF period; it is the number of RF cycles for any disturbance to fall to $e^{-\pi} \approx 4\%$ of its initial value. Hence the filling time is 250 μs , or more, in our high-Q scenario. This should be compared with the revolution period, for a 2 km ring and light-speed particles, which is 6.7 μs . Evidently, the cavity phase cannot be made to follow the ideal variation on a turn-by-turn basis. One could imagine a vector feedback of the gap voltage so as to reduce the filling time by say a factor 20, but this would still not guarantee sufficient waveform fidelity and moreover the peak power would rise.

One way to lower the R and the Q, without increasing the RF power, would be to accelerate more slowly over more turns of the ring, but this results in greater muon decay losses and probably smaller longitudinal acceptance. If superconducting cavities were used, the power argument does not apply; but with quality factors from 10^6 to 10^9 pure sinusoid operation is the only mode possible.

2 RF waveform scenarios

2.1 Single frequency, fixed phases

One can imagine to operate all the cavities at a single frequency. If no care is paid, then acceleration will be stochastic. However, one may pick the initial individual cavity phases and optimize the single fixed frequency; and then some net acceleration will result. Let T be the desired crossing time corresponding to zero phase angle. The phases are easily set with an In-phase and Quadrature (IQ) mixer based on the following decomposition:

$$\cos \omega(t - T) = \cos \omega t \cos \omega T + \sin \omega t \sin \omega T . \quad (1)$$

2.2 Moving phases

One can imagine to move the phases of accelerating stations on a turn-by-turn basis. There are two ways in which this may be achieved. Unfortunately, use of either of them would entail use of all (and more) of the available space for RF in the ring!

2.2.1 Multiple frequencies

Let us suppose that the ideal phase variation $\Delta\Phi(t)$ is known with respect to some carrier frequency ω . Further, let this ideal variation be approximated by the function

$$\Delta\Phi(t) \approx \Phi + \Delta\phi \cos(\Omega t + \phi) , \quad (2)$$

where the parameters Φ , $\Delta\phi$, Ω and ϕ are obtained by fitting. Now this may be expanded in the form

$$\cos(\omega t + \Phi) \cos[\Delta\phi \cos(\Omega t + \phi)] - \sin(\omega t + \Phi) \sin[\Delta\phi \cos(\Omega t + \phi)] . \quad (3)$$

A low order Fourier-Bessel expansion then gives:

$$\cos(\omega t + \Phi) J_0(\Delta\phi) - 2J_1(\Delta\phi) \sin(\omega t + \Phi) \cos(\Omega t + \phi) - 2J_2(\Delta\phi) \cos(\omega t + \Phi) \cos 2(\Omega t + \phi) . \quad (4)$$

Under the assumption that $\Delta\phi$ is small, the J_0 and J_1 Bessel function terms dominate; and we are left with a constant in-phase term and a modulated quadrature term, respectively. The quadrature term may be generated either by a modulated low-quality-factor system or by synthesis of two sinusoids generated by high-quality-factor systems.

$$2 \sin(\omega t + \Phi) \cos(\Omega t + \phi) = \sin[(\omega + \Omega)t + \Phi + \phi] + \sin[(\omega - \Omega)t + \Phi - \phi] . \quad (5)$$

Hence, three frequencies are required: a carrier ω and lower and upper sidebands $\omega \pm \Omega$. We have carried out this procedure with the conclusion that the $J_1(\Delta\phi)$ correction terms are not small. To sweep the phase correctly requires a quadrature modulation term comparable with the in-phase carrier. Note, so many approximations are made in this derivation that it would probably be better to do numerical fitting of three arbitrary sinusoids to the known function $\cos[\omega t + \Delta\Phi(t)]$.

2.2.2 IQ corrector

The desired waveform may be written in IQ form:

$$\cos[\omega t + \Delta\Phi(t)] = \cos(\omega t) + [\cos \Delta\Phi(t) - 1] \cos(\omega t) - \sin \Delta\Phi(t) \sin(\omega t) . \quad (6)$$

One may generate the first term with the high-Q, high-R RF, and the second two terms, involving $\Delta\Phi(t)$, with a low-Q, low-R frequency agile system. If $\Delta\Phi(t)$ is a small variation, then the time-varying amplitudes $\sin \Delta\Phi$ and $[\cos \Delta\Phi - 1]$ are small; and one could imagine to generate them with a low-Q cavity. For the muon-FFAG, unfortunately, the peak values of the quadrature term are comparable with the carrier; and so high instantaneous power is required. Nevertheless, this scheme certainly has the merit of flexibility.

A drawback of this scheme is that it can only be made to work if the bunch train does not fill the entire machine circumference and the cavity filling time is shorter than the gap. The desired quality factor is equal to the number of empty RF periods and could be as high as 10^3 . The cavity phases are reset (i.e. non-integer harmonic operation) during the passage of the beam gap. Simulation of the beam dynamics for such a scenario requires modeling of the transient response of the cavities; this is discussed below in section 11.

2.3 Ideal phases

Let us set aside for a moment the technological problems, and assume the ideal phases can be provided. The question then becomes “what longitudinal phase space is generated?”, and how is it affected by the addition of second harmonic.

2.4 Dual harmonic

One may imagine to flat-top the RF waveform by the addition of 2nd harmonic. We have used the following waveform:

$$(1/3)[4 \cos \omega t - \cos 2\omega t], \quad (7)$$

and so a 33% over-voltage is required at the fundamental.

2.5 Choice of RF

For bunches of given time and energy spread, the phase variation across the bunch is smaller if the RF is lower. Hence an alternative to flat-topping with 2nd harmonic would be to use a lower fundamental frequency, say 100 MHz, as a means to achieving greater longitudinal acceptance.

For a given cavity quality factor, the time to re-adjust the cavity phases becomes doubled when 100 Mhz is used; and so the bunch train must be shortened. However, this is not a concern if one adopts the “single frequency, fixed-phases strategy” and makes no attempt to adjust phases turn-by-turn.

Due to the larger physical size of 100 MHz cavities and the Kilpatrick scaling on gap breakdown voltage, the average gradient attainable with lower frequency cavities is likely to be unfavourable compared with 200 MHz operation. However, if use of lower RF facilitates acceleration over a larger number of turns, the lower gradient is less of an issue.

3 Optimization Strategy

Let us first say that there are probably many possible optimization strategies, and that we report only one of them. Our optimization is based on reference particles (one per bunch), not on complete bunches/ensembles and so cannot directly be used to maximize input acceptance or minimize output emittance.

Initially, the ideal phases cavity-by-cavity and turn-by-turn are calculated for a single synchronous particle in the reference bunch. One assumes this particle is accelerated perfectly at every cavity, and adjusts the phases to make this possible. The ideal phases and gap-crossing times are recorded.

Note, we choose to arrange all the ideal phases so that at the gap-crossing time the phase is zero and the reference particle always rides the crest of the wave. This not only maximizes acceleration but also minimizes the transverse (nonlinear) defocusing of the RF gap. Hopefully, this “zero-phase decision” feeds down to the less ideal RF scenarios discussed below. Most probably the parabolic acceptance area seen in many of the cases studied stems from this decision.

3.1 Ideal phases

The ideal phases for a single reference bunch are known; but one must also consider other bunches in the train. We assume that the RF system is not sufficiently agile to make adjustments for individual bunches, but rather that it runs at constant frequency during the train and that phase adjustments are made in the beam gap. Probably the best solution is to have different constant frequencies on each turn, but we chose a simpler option: to use the “best frequency” found above. This also simplifies the IQ-corrector concept because there is a single carrier frequency.

3.2 Fixed frequency and phases

To optimize the fixed frequency and phases, one chooses a frequency and then calculates the phases at the gap-crossing times of the ideal particle. One then forms the root-mean-square deviation of the fixed-phases from the ideal values. Then a search is made to find the “best frequency” which minimizes this r.m.s. phase deviation. The results of this calculation is a set of “best phases” for the reference bunch; these phases are not-ideal.

Because every bunch arrives displaced from the ideal phase, we must find some way of accelerating that is tolerant of poor phasing.

3.3 Over-voltages

Since the time of Veskler and McMillan, it has been recognized as advantageous to use an “over-voltage”. Rather than accelerate at the crest of the RF wave, one lets the ideal particle lag or lead the wave and increases the voltage to compensate. In a synchrotron, the advantage of increasing the phase space area that may be accelerated more than compensates for the penalty of higher voltage. In a muon FFAG the benefit is less clear, *a priori*, because of the speed and path length variations. However, *a posteriori*, modest over-voltage is of enormous benefit; but it is not a “cure all”.

3.3.1 Fixed frequency and phases

We chose to pick the over-voltage so as to minimize the bunch-to-bunch variation of the extraction energy. We do this by tracking a reference particle in each bunch of the train and using a numerical search for the best voltage. Though synchronous phase has little meaning in a muon FFAG, nevertheless one can define a quantity that satisfies $\text{over-voltage} \times \cos(\phi_s) = \text{nominal-voltage}$.

3.3.2 Ideal phases

One may wonder if allowing an additional small turn-by-turn phase variation can reduce the bunch-to-bunch energy variation at extraction. A small over-voltage is then needed to compensate for the “synchronous phase program”.

4 Simulations of longitudinal dynamics

The model used is very simple. One assumes *complete* decoupling from the transverse motion! Then we break the 2 km ring into roughly 300 identical cells and lump an RF station (could be 1 or more cavities) in each cell. Cavities all run at the same frequency, but can have individual phases. The arrival time depends on $\beta = v/c$ and path length. A parabola has been fitted through Carol Johnson's delta-circumference versus energy plot and is used for the path length computation. I assume that the energy acceptance is 6-to-20 GeV $\pm 10\%$ of injection and extraction energies. Typically we track 100 bunches, with roughly 1000 particle per bunch.

Initially, the longitudinal phase plane is uniformly flooded with trial particles; and one attempts to accelerate them. Particles which survive the complete acceleration to 20 GeV are recorded and used to map out both the input admittance and the output emittance. To increase accuracy, the procedure is repeated using the admittance of the previous trial as a basis for populating the input ensemble of the subsequent trial. Because the input beam is assumed to have an energy spread of $\pm 10\%$, the input admittance is truncated to an energy band $\pm 10\%$ wide.

4.1 Summary of cases versus RF requirements

Cases #	turns %	$\Delta E/\text{turn}$ GeV	$\Delta E/\text{cell}$ MeV	$\langle \text{gradient} \rangle$ MeV/metre	RF MHz
1,2,3,4	5	2.8	9.333	2.80	200
5,6,7,8,9,10,11,12,13,36	5	2.8	9.333	1.40	200
14,15,16,17,18,19,30,32,33	10	1.4	4.667	0.70	200
20,21,23,25	7	2.0	6.667	1.00	200
22,24	6	2.33	7.777	1.167	200
26,31	10	1.4	4.667	0.70	100
27	7	2.0	6.667	1.00	100
28	8	1.75	5.833	.875	100
29	9	1.56	5.185	.7778	100
34	5	2.8	9.333	1.40	100

5 Summary tables

It is useful to give more than one measure of bunch size in the longitudinal phase plane; and so, in addition to input acceptance and output emittance, we provide average, full-width and r.m.s. indicators of bunch phase-length and energy width. In addition, there are bunch to bunch variations; and to give some idea of this variability we provide average and peak values along the bunch train. This data is tabulated below.

5.1 Symbols in the tables

Cs = Case, G = single frequency and fixed phases, E = exact phases set turn-by-turn, D = dual harmonic operation. The bra-kets, $\langle \dots \rangle$ denote statistical averaging over the bunch train. The

use of accents \checkmark and $\hat{\cdot}$ denotes a sorting through the bunch train to find minimum and maximum values, respectively.

$\langle \text{input} \rangle$ = average bunch input admittance

$\langle \text{output} \rangle$ = average bunch output emittance

in-min/max = minimum/maximum input admittance in the bunch train

ot-min/max = minimum/maximum output emittance in the bunch train

$\Delta \check{E}$ = lowest centroid-energy deviation in the bunch train

$\Delta \hat{E}$ = highest centroid-energy deviation in the bunch train

$\langle \bar{\phi} \rangle$ = average bunch centroid phase

$\langle \phi_{FW} \rangle$ = average bunch full-width phase spread

$\langle \bar{E} \rangle$ = average bunch centroid energy

$\langle E_{FW} \rangle$ = average bunch full-width energy spread

$\langle \text{rms} \phi \rangle$ = average root-mean-square bunch phase spread

$\langle \text{rms} E \rangle$ = average root-mean-square bunch energy spread

$\check{\phi}_{FW}$ = lowest full-width phase spread

$\hat{\phi}_{FW}$ = highest full-width phase spread

\check{E}_{FW} = lowest full-width energy spread

\hat{E}_{FW} = highest full-width energy spread

$\check{\phi}_{\text{rms}}$ = lowest r.m.s. phase spread

$\hat{\phi}_{\text{rms}}$ = highest r.m.s. phase spread

\check{E}_{rms} = lowest r.m.s. energy spread

\hat{E}_{rms} = highest r.m.s. energy spread

5.2 Summary of Results for 200 MHz RF

Cs #	G	E	D	ϕ_s deg	overV	Cc km	trn #	$\langle \text{input} \rangle$ eV.s	$\langle \text{output} \rangle$ eV.s	in-min eV.s	in-max eV.s	ot-min eV.s	ot-max eV.s	$\Delta \hat{E}$ MeV	$\Delta \hat{E}$ MeV
3	Y	N	N	N	N	1	5	zero	zero	0	0	0	0	-4786.	-4683.
4	Y	N	Y	N	N	1	5	0.337	0.337	.3358	.3374	.3354	.3375	-2209.	-2195.
1	Y	N	N	-40.67	1.318	1	5	1.635	1.832	1.627	1.639	1.770	1.938	-20.7	+17.0
2	Y	N	Y	-34.5	1.213	1	5	2.142	2.229	2.136	2.147	2.138	2.372	-7.5	+6.5
6	N	Y	N	N	N	2	5	1.223	1.535	1.218	1.228	1.487	1.592	-3.2	-.095
5	N	Y	Y	N	N	2	5	2.212	2.513	2.205	2.221	2.460	2.571	-.095	+.095
7	N	Y	N	Y,P	1.0003	2	5	1.192	1.515	1.182	1.200	1.466	1.554	-1.3	+0.87
11	N	Y	Y	Y,P	1.0002	2	5	2.213	2.503	2.202	2.219	2.444	2.547	+1.85	+1.85
36	N	Y	N	Y,P	Y,1.20	2	5	0.8470	0.8230	0.8435	0.8494	0.8194	0.8259	-77.1	+75.6
12	Y	N	N	N	N	2	5	zero	zero	0	0	0	0	-11673	-11357
10	Y	N	Y	N	N	2	5	0.2322	0.2323	0.2307	0.2330	0.2306	0.2332	-2413.	-2390.
8	Y	N	N	-41.25	1.330	2	5	1.405	1.914	1.399	1.411	1.840	2.035	-28.	+40.
9	Y	N	Y	-34.46	1.213	2	5	1.989	2.264	1.982	1.994	2.167	2.336	-16.6	+16.7
13	Y	N	Y	-34.46	1.213	2	5	1.947	2.2714	1.935	1.964	2.1913	2.375	-88.8	+81.2
33	N	Y	N	N	Y,1.30	2	10	1.632	19.68	1.613	1.646	17.64	22.49	-5925	-5643
14	N	Y	N	N	N	2	10	0.4968	0.6986	0.4793	0.5193	0.6372	0.8707	-3.2	.007
19	N	Y	Y	N	N	2	10	1.699	2.057	1.668	1.733	1.878	2.367	.007	.007
15	Y	N	N	N	N	2	10	zero	zero	0	0	0	0	-13533	-13497
16	Y	N	Y	N	N	2	10	zero	zero	0	0	0	0	-13578	-13545
17	Y	N	N	16.10	1.041	2	10	zero	zero	0	0	0	0	-13431	-13414
18	Y	N	Y	2.04	1.0006	2	10	zero	zero	0	0	0	0	-13564	-13540
30	Y	N	N	N	Y,1.30	2	10	zero	zero	0	0	0	0	-14338	-14333
32	Y	N	Y	N	Y,1.30	2	10	zero	zero	0	0	0	0	-14083	-13774
20	Y	N	N	24.91	1.103	2	8	zero	zero	0	0	0	0	-13591	-13522
25	Y	N	N	-45.0	1.414	2	7	0.1678	0.1639	0.1670	0.1687	0.1630	0.1653	-12761	-12696
24	Y	N	N	40.49	1.319	2	6	0.3283	0.3229	.3273	.3302	.3216	.3255	-11111	-11080
21	Y	N	Y	19.91	1.064	2	8	.0385	.0406	.0327	.0446	.0343	.0472	-11644	-11564
23	Y	N	Y	33.19	1.195	2	7	0.3086	0.3082	.3078	.3098	.3074	.3093	-10442	-10404
22	Y	N	Y	44.40	1.400	2	6	1.706	1.884	1.701	1.712	1.833	1.935	-9.2	+8.8

Case #13 is 400 bunches. All other cases use 100 bunches.

5.2.1 Input statistics

Cs #	$\langle\bar{\phi}\rangle$ deg	$\langle\phi_{FW}\rangle$ deg	$\langle\bar{E}\rangle$ GeV	$\langle E_{FW}\rangle$ GeV	$\langle rms\phi\rangle$ deg	$\langle rmsE\rangle$ GeV	$\hat{\phi}_{FW}$ deg	$\hat{\phi}_{FW}$ deg	\hat{E}_{FW} GeV	\hat{E}_{FW} GeV	$\hat{\phi}_{rms}$ deg	$\hat{\phi}_{rms}$ deg	\hat{E}_{rms} GeV	\hat{E}_{rms} GeV
4	-83.23	76.54	6.4116	0.4666	18.472	0.1253	76.532	76.537	0.4666	0.4666	18.426	18.532	0.1250	0.1255
1	-65.39	153.5	6.1325	1.1686	35.406	0.3146	153.48	153.49	1.1686	1.1686	35.281	35.477	0.3141	0.3151
2	-69.43	178.2	6.0881	1.20	42.303	0.3377	174.42	179.14	1.20	1.20	42.241	42.446	0.3373	0.3381
6	-4.395	122.9	5.9799	1.20	30.821	0.3186	121.10	124.47	1.20	1.20	30.717	30.973	0.3177	0.3194
5	-0.3516	182.8	5.9791	1.20	47.304	0.3337	182.74	183.84	1.20	1.20	47.111	47.535	0.3333	0.3342
7	5.449	122.5	5.9757	1.20	30.570	0.3194	121.10	124.47	1.20	1.20	30.425	30.699	0.3185	0.3201
11	-1.230	181.5	5.9803	1.20	47.201	0.3337	179.13	183.85	1.20	1.20	46.916	47.417	0.3333	0.3341
36	51.72	106.34	6.2530	0.8761	24.81	0.2343	104.9	107.8	0.8761	0.8761	24.73	24.88	0.2335	0.2350
10	32.87	63.58	6.4396	0.3972	15.478	0.1058	62.434	64.448	0.3872	0.3976	15.340	15.609	0.1055	0.1064
8	48.87	147.3	6.1919	1.0224	34.861	0.2732	145.40	149.45	1.0224	1.0224	34.778	34.949	0.2718	0.2742
9	41.31	174.8	6.1131	1.20	41.357	0.3253	174.42	179.13	1.20	1.20	41.234	41.442	0.3247	0.3262
13	52.03	176.6	6.1219	1.1686	41.235	0.3212	174.42	179.14	1.1686	1.1686	41.10	41.41	0.3199	0.3222
14	81.56	105.16	6.0723	0.9412	27.50	0.2370	101.99	107.82	0.9346	0.9639	27.25	27.85	0.2356	0.2387
19	64.7	175.4	6.0175	1.20	47.42	0.3226	174.4	179.1	1.20	1.20	47.25	47.59	0.3211	0.3242
25	123.9	78.75	6.5067	0.2326	18.23	.0629	78.37	80.60	0.2361	0.2361	18.18	18.31	.06265	.06316
24	17.7	95.09	6.4501	0.3789	22.19	0.1012	93.633	96.80	0.3789	0.3789	22.15	22.27	0.1008	0.1014
21	24.6	34.20	6.5511	0.1209	8.401	.03263	32.00	36.76	.1097	.1300	7.808	8.884	.0299	.0352
23	37.8	99.49	6.4637	0.3406	22.80	.0922	99.49	99.49	.3406	.3406	22.90	23.07	.0918	.0923
22	5.5	173.9	6.1713	1.081	40.40	0.2897	169.7	174.4	1.081	1.081	40.31	40.56	.2891	.2904

6

5.2.2 Output statistics

Cs #	$\langle\bar{\phi}\rangle$ deg	$\langle\phi_{FW}\rangle$ deg	$\langle\bar{E}\rangle$ GeV	$\langle E_{FW}\rangle$ GeV	$\langle rms\phi\rangle$ deg	$\langle rmsE\rangle$ GeV	$\check{\phi}_{FW}$ deg	$\hat{\phi}_{FW}$ deg	\check{E}_{FW} GeV	\hat{E}_{FW} GeV	$\check{\phi}_{rms}$ deg	$\hat{\phi}_{rms}$ deg	\check{E}_{rms} GeV	\hat{E}_{rms} GeV
4	-45.04	62.31	18.234	0.5538	16.759	0.1494	61.804	62.590	0.55316	0.55442	15.209	22.108	0.1491	0.1496
1	50.80	100.89	19.764	2.8386	24.730	0.7050	99.122	102.53	2.8155	2.8500	24.576	25.084	0.6979	0.7086
2	35.48	109.94	19.759	2.9131	28.742	0.6332	108.29	112.22	2.8678	2.9343	28.071	30.659	0.6306	0.6382
6	-30.64	100.87	19.070	2.4392	25.296	0.6655	99.246	102.13	2.4268	2.4459	23.621	28.653	0.6627	0.6685
5	-27.50	147.49	19.336	2.5936	41.356	0.7355	145.86	148.48	2.5861	2.5963	38.689	48.215	0.7330	0.7382
7	-29.85	99.76	19.070	2.4589	25.408	0.6701	97.937	101.34	2.444	2.463	23.377	28.691	0.6671	0.6732
11	-28.02	148.18	19.34	2.596	41.756	0.7339	146.12	149.52	2.5918	2.5986	38.809	49.100	0.7294	0.7371
36	29.83	108.0	20.409	3.9112	28.82	1.0965	107.3	108.7	3.895	3.917	28.75	28.87	1.091	1.102
10	-47.40	52.12	18.199	0.4771	18.415	0.1274	51.325	52.635	.47638	.47796	12.321	27.011	0.1266	0.1280
8	44.25	82.77	19.947	3.2453	23.831	0.8186	81.963	84.320	3.200	3.2556	21.647	32.130	0.8067	0.8274
9	27.50	111.10	19.753	3.0175	28.221	0.6747	109.46	112.34	2.9927	3.0306	25.395	38.063	0.6705	0.6800
13	42.95	98.837	19.853	3.0585	26.853	0.6763	92.18	101.86	2.9753	3.101	23.33	38.06	0.6709	0.6846
14	-15.71	78.99	19.399	2.2563	20.714	0.5488	74.893	82.22	2.2114	2.2744	15.90	32.21	0.5383	0.5661
19	-15.71	124.3	19.527	2.525	38.02	0.5628	119.93	126.74	2.449	2.549	27.57	55.42	0.5468	0.5807
25	35.04	63.56	19.137	1.9627	17.12	0.5495	63.01	63.92	1.953	1.966	17.06	17.17	0.5453	0.5528
24	-46.59	57.70	19.200	2.104	14.95	0.5833	57.25	58.17	2.092	2.106	14.90	14.10	0.5792	0.5862
21	-95.84	17.50	18.10	0.2420	18.38	.06408	15.97	18.85	.2199	.2650	4.120	50.86	.05827	.06918
23	-58.52	29.03	18.619	1.224	7.180	0.3282	28.96	29.08	1.219	1.226	7.165	7.193	0.3272	0.3297
22	11.60	109.15	20.073	3.2669	27.46	0.6848	108.0	110.3	3.228	3.287	27.32	27.60	0.6768	0.6932

5.3 Summary of Results for 100 MHz RF

Cs	G	E	D	ϕ_s	overV	Cc	trn	$\langle input\rangle$	$\langle output\rangle$	in-min	in-max	ot-min	ot-max	$\Delta\check{E}$	$\Delta\hat{E}$
26	Y	N	N	15.23	1.0374	2	10	zero	zero	0	0	0	0	-13392	-13069
31	Y	N	N	N	Y,1.30	2	10	1.838	1.795	1.834	1.842	1.790	1.800	-560.	-550.
29	Y	N	N	-41.22	1.329	2	9	2.994	2.924	2.986	3.008	2.912	2.938	-38.1	+37.2
28	Y	N	N	-37.65	1.263	2	8	3.245	3.178	3.234	3.259	3.166	3.193	-30.5	+30.0
27	Y	N	N	-35.60	1.230	2	7	3.685	3.630	3.675	3.697	3.616	3.642	-29.5	+29.4
34	Y	N	N	-36.93	1.251	2	5	3.699	3.609	3.686	3.714	3.595	3.632	-69.8	+69.7

5.3.1 Input statistics

Cs #	$\langle\bar{\phi}\rangle$ deg	$\langle\phi_{FW}\rangle$ deg	$\langle\bar{E}\rangle$ GeV	$\langle E_{FW}\rangle$ GeV	$\langle\text{rms}\phi\rangle$ deg	$\langle\text{rms}E\rangle$ GeV	$\check{\phi}_{FW}$ deg	$\hat{\phi}_{FW}$ deg	\check{E}_{FW} GeV	\hat{E}_{FW} GeV	$\check{\phi}_{\text{rms}}$ deg	$\hat{\phi}_{\text{rms}}$ deg	\check{E}_{rms} GeV	\hat{E}_{rms} GeV
31	30.0	130.9	6.2957	0.7591	30.56	0.2049	129.2	132.8	0.7591	0.7591	30.48	30.63	0.2045	0.2052
29	56.8	153.2	6.1718	1.0809	35.37	0.2885	149.4	153.5	1.081	1.081	35.26	35.46	0.2876	0.2894
28	46.7	151.2	6.1338	1.1686	35.24	0.3134	149.2	153.5	1.169	1.169	35.14	35.34	0.3123	0.3139
27	36.6	151.3	6.0916	1.20	36.60	0.3334	149.2	153.5	1.20	1.20	36.50	36.70	0.3328	0.3343
34	29.75	161.7	5.9957	1.20	39.16	0.3237	161.6	162.0	1.20	1.20	39.07	39.26	0.3232	0.3242

5.3.2 Output statistics

Cs	$\langle\bar{\phi}\rangle$	$\langle\phi_{FW}\rangle$	$\langle\bar{E}\rangle$	$\langle E_{FW}\rangle$	$\langle\text{rms}\phi\rangle$	$\langle\text{rms}E\rangle$	$\check{\phi}_{FW}$	$\hat{\phi}_{FW}$	\check{E}_{FW}	\hat{E}_{FW}	$\check{\phi}_{\text{rms}}$	$\hat{\phi}_{\text{rms}}$	\check{E}_{rms}	\hat{E}_{rms}
31	4.227	69.44	19.633	2.736	16.93	0.7273	69.10	69.97	2.718	2.742	16.90	16.96	0.7237	0.7310
29	54.11	86.73	19.974	3.204	21.39	0.8168	86.60	86.79	3.176	3.212	21.38	21.41	0.8120	0.8254
28	42.17	84.17	19.76	3.143	19.13	0.8082	84.03	84.27	3.118	3.151	19.11	19.15	0.8057	0.8130
27	34.39	91.29	19.659	3.1976	20.57	0.8016	91.25	91.32	3.176	3.207	20.54	20.59	0.7979	0.8945
34	34.38	116.6	20.106	3.9927	31.96	1.198	115.7	117.8	3.986	3.999	31.91	32.04	1.195	1.203

6 5-turns, 200 MHz acceleration results

6.1 Single frequency

We shall consider acceleration in five (5) turns of the FFAG. If one uses a single (but optimal) frequency, fixed initial cavity phases and the nominal RF voltage, then the desired acceleration is not achieved (case #12); a tiny fraction of particles reach 15.25 GeV.

If one adds 2nd harmonic (case #10), a small phase space area of 0.23 eV.s is transported to 17.6 GeV and there is no emittance growth.

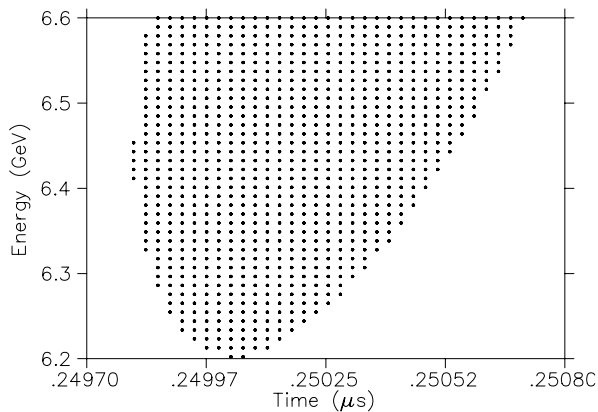


Figure 1: $\pm 10\%$ band from Input Acceptance

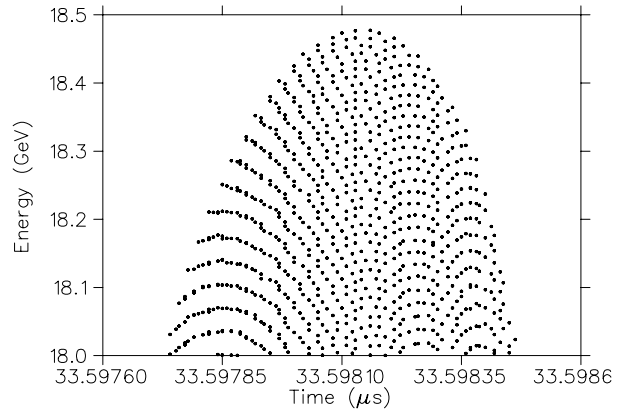


Figure 2: Maps to the Output Emittance, Case #10. Dual harmonic.

6.1.1 With over-voltage

However, if one allows a 33% over-voltage (case #8) then an input phase space area (admittance) of 1.41 eV.s is transported from 6 to 20 GeV by which time the emittance has increased to 1.91 eV.s. There is no need to adjust the phasing, the beam will find for itself the “right place”; but we can calculate the phase at injection for synchronization purposes.

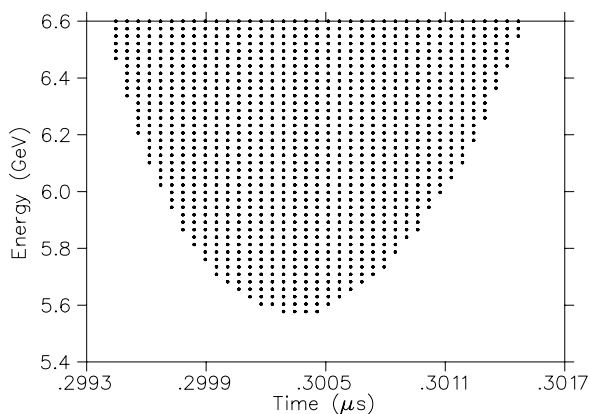


Figure 3: $\pm 10\%$ band from Input Acceptance

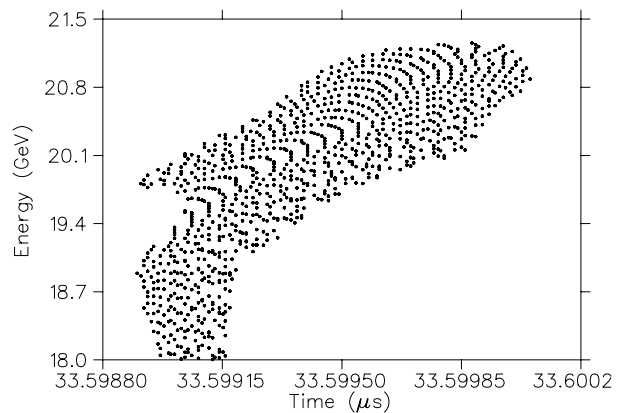


Figure 4: Maps to the Output Emittance, Case #8. Single harmonic.

If one adds second harmonic (case #9), then one needs 1.333×1.213 of the nominal voltage. The admittance rises to 1.99 eV.s and the output emittance is 2.26 eV.s. As will be noted in the figures, transport is non-linear and the occupied phase space has a bizarre shape.

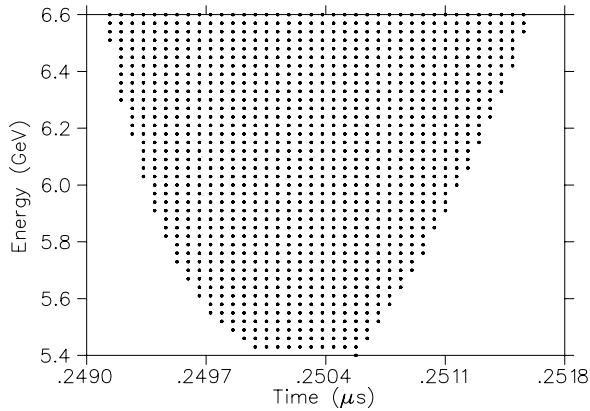


Figure 5: $\pm 10\%$ band from Input Acceptance

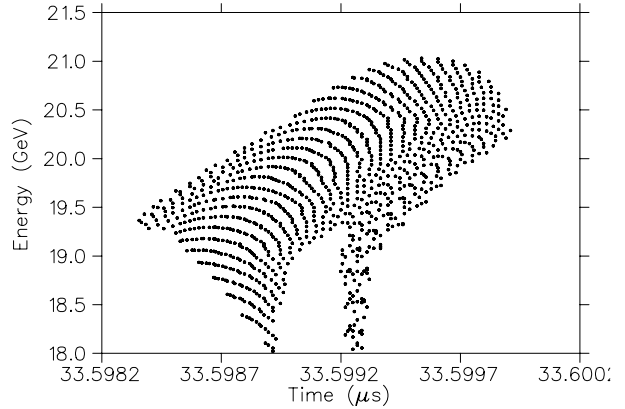


Figure 6: Maps to the Output Emittance, Case #9. Dual harmonic.

If one uses identical parameters but considers 400 bunches (case #13), rather than 100, then one finds some small degradation of the beam quality. The input admittance falls to 1.95 eV.s and the output emittance rises to 2.27 eV.s. Further, the bunch-to-bunch energy variation rises from ± 17 to ± 85 MeV.

6.2 Ideal phases

When the ideal phasing is used, and no other measures are taken (case #6), an input admittance of 1.22 eV.s is successfully accelerated to 20 GeV with an output emittance of 1.535 eV.s. Notice, that despite the ideal phasing, the transport is non-linear.

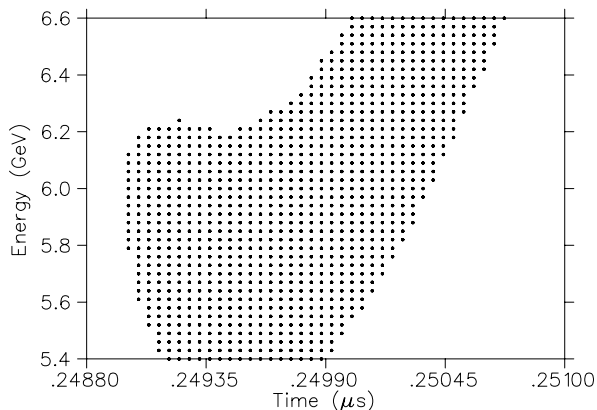


Figure 7: $\pm 10\%$ band from Input Acceptance

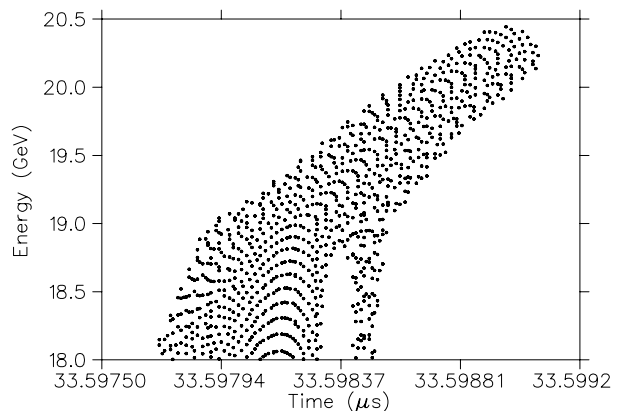


Figure 8: Maps to the Output Emittance, Case #6. No over voltage.

If one allows a tiny variation of the synchronous phase (case #7), then the bunch-to-bunch energy variation can be reduced from -3 to ± 1 MeV; but at the cost of a small degradation in input admittance 1.19 eV.s

If one adds second harmonic to the basic scheme (case #5), then the input admittance rises to 2.21 eV.s and the output emittance becomes 2.51 eV.s. However, the transport is so non-linear that the useful phase space area is probably only one half of these values. Perhaps the situation could be improved by adjusting the phase of the second harmonic.

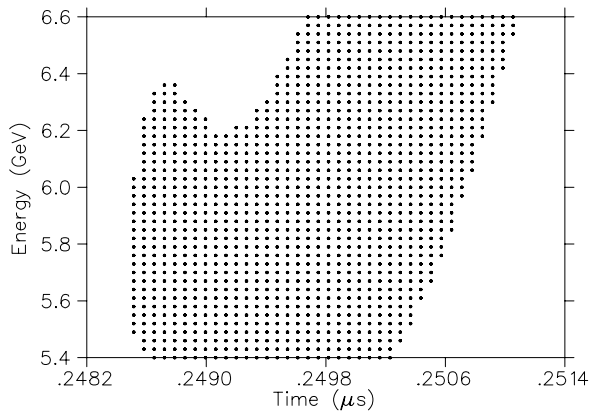


Figure 9: $\pm 10\%$ band from Input Acceptance

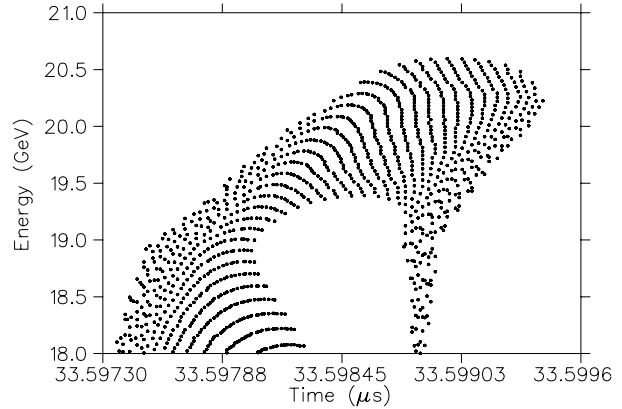


Figure 10: Maps to the Output Emittance, Case #5. Dual harmonic.

Allowing a tiny phase variation (case #11) results in a 10^{-4} increase in input admittance, but increases the bunch-to-bunch energy spread to ± 1.9 MeV.

6.2.1 Over-voltage

It is salutary to observe that imposing a 20% over voltage results in a decrease in transmission; compare case 6 (1.22 eV.s) with case 36 (0.85 eV.s) below.

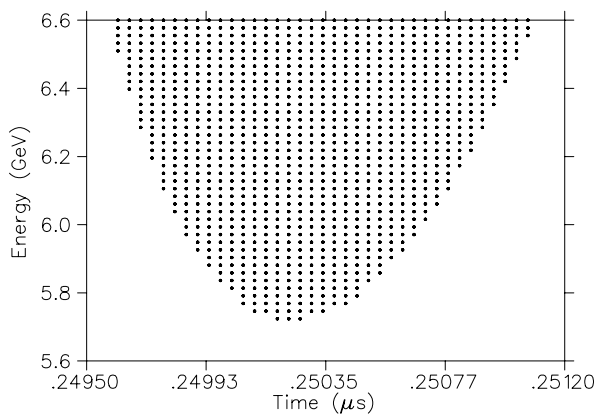


Figure 11: $\pm 10\%$ band from Input Acceptance

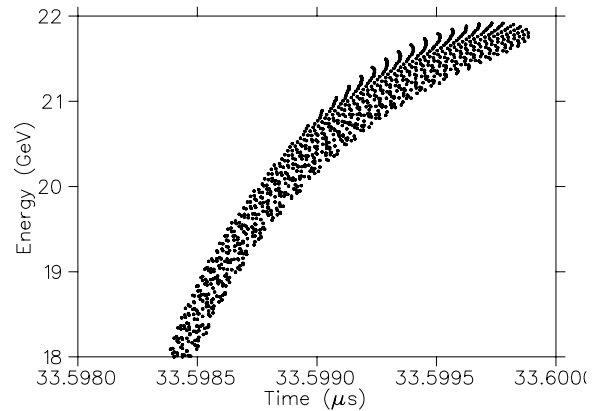


Figure 12: Maps to the Output Emittance, Case #36. 20% over-voltage.

6.3 Conclusion

For 5-turn acceleration, there is little difference in the output emittance between the use of “ideal phases” versus using a combination of “best phases” and an over-voltage. When 2nd harmonic is employed, the useful acceptance is probably greater when the “single-frequency” scenario is adopted.

7 Other than five turns

To first order, the phase slippage will increase linearly with time; but the RF waveform $\cos(\omega t)$ is of approximately parabolic dependence about the peak, and so one expects the transmission to fall in a roughly parabolic manner as the number of turns is increased.

7.1 Single frequency

This trend is displayed in cases 24,25,20 (single harmonic) and cases 22,23,21 (dual harmonic). The addition of 2nd harmonic (and greater over-voltage) is rather beneficial; compare cases 22 versus 24 which are both for 6-turn acceleration.

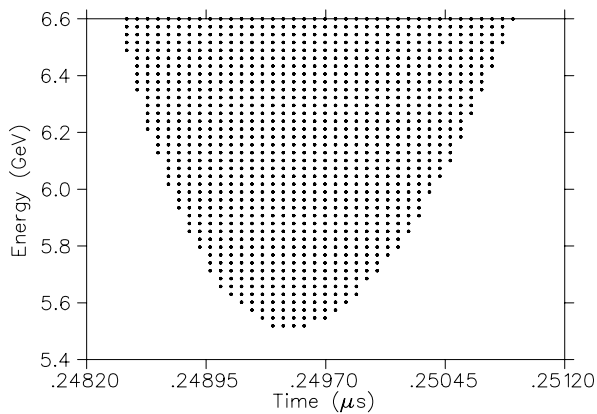


Figure 13: $\pm 10\%$ band from Input Acceptance

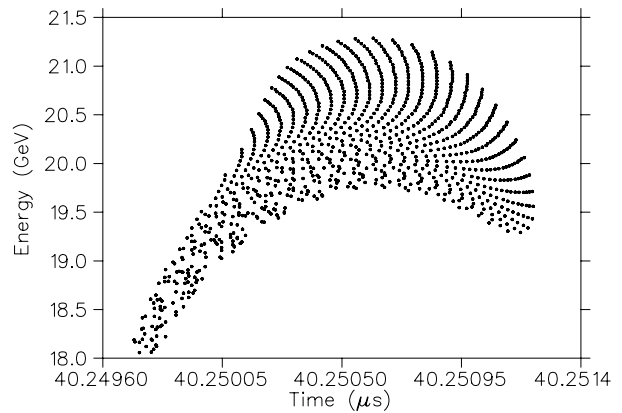


Figure 14: Maps to the Output Emittance, Case #22. Dual harmonic.

In case 24, a $1.3\times$ over voltage factor and single harmonic is used to provide an input admittance and output emittance of 0.3 eV.s. In case 22, a 1.40×1.33 over voltage and dual harmonic is used to achieve an input admittance of 1.7 eV.s and output emittance of 1.9 eV.s.

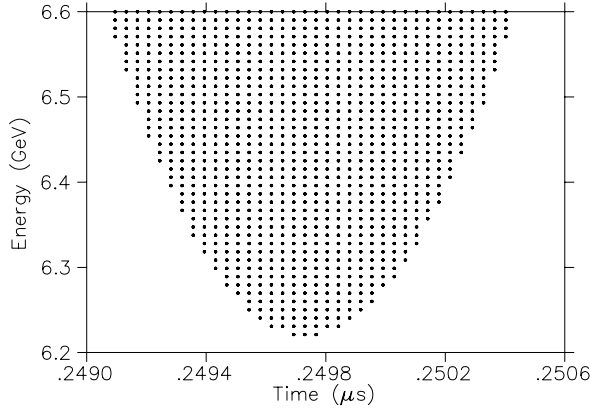


Figure 15: $\pm 10\%$ band from Input Acceptance

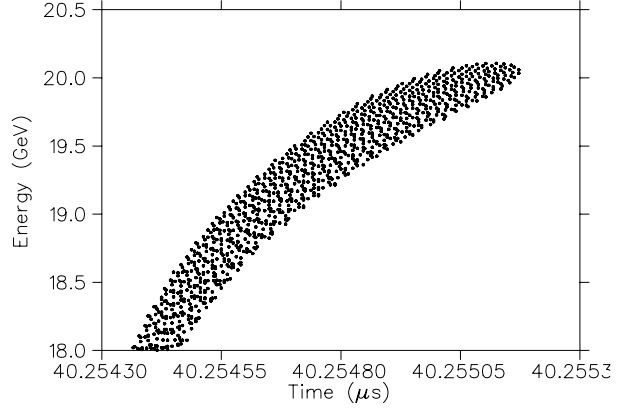


Figure 16: Maps to the Output Emittance, Case #24. Single harmonic.

Notice that the constrained optimization procedure that we have employed which couples over-voltage with synchronous phase has a tendency to use lower over-voltages, the greater is the number of turns; and some loss in transmission can be ascribed to this. See cases 24,25,20 where the over-voltage drops from 1.4 to 1.1 and the admittance falls progressively from 0.328 eV.s to zero as the number of turns is increased from six to eight.

7.2 10-turns

We have not achieved successful acceleration over ten (10) turns with 200 MHz RF unless the ideal phases are used. Compare cases 15,16,17,18,30,32 (fixed phases) with cases 14,19 (ideal phases).

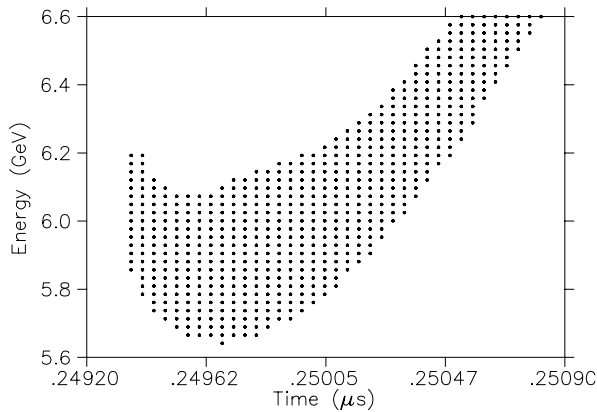


Figure 17: $\pm 10\%$ band from Input Acceptance

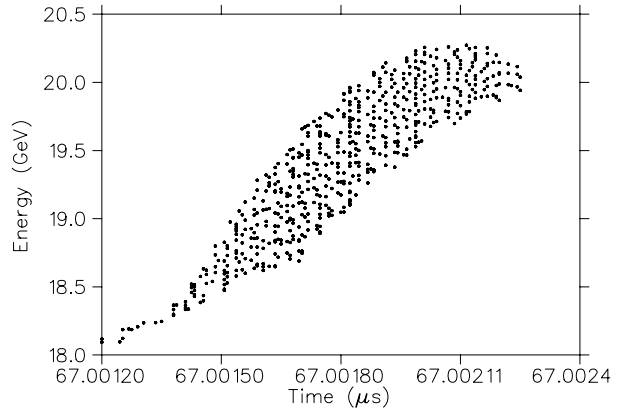


Figure 18: Maps to the Output Emittance, Case #14. Ideal phases, dual harmonic.

When ideal-phases and single-harmonic is used for 10-turn acceleration, case 14, the admittance falls by about 50% compared with 5-turns. The addition of second harmonic, case 19, restores the admittance to within 25% of the 5-turn value.

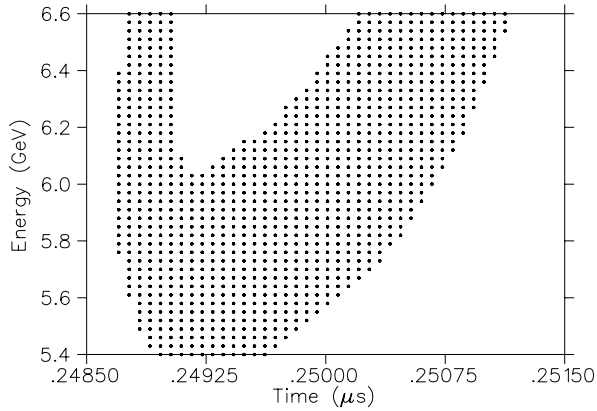


Figure 19: $\pm 10\%$ band from Input Acceptance

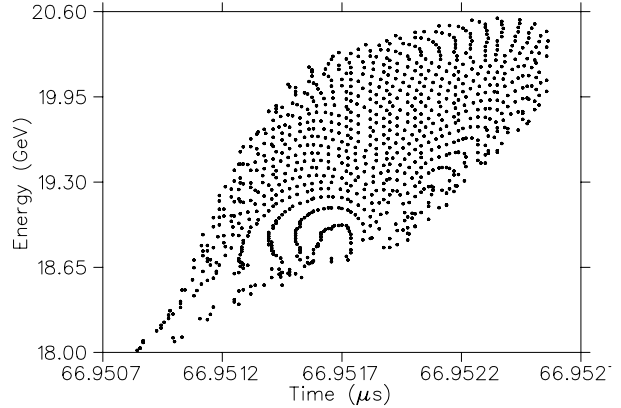


Figure 20: Maps to the Output Emittance, Case #19. Ideal phases, dual harmonic.

It is interesting to note that it is not a straight forward matter to compensate the admittance loss by increasing the over-voltage. In case 33, the addition of a 30% over-voltage (c.f. case 14) leads to a very substantial emittance growth due to excessive filamentation. The input emittance is 1.6 eV.s whereas the output emittance (i.e. the “enclosed area”) is 19.6 eV.s!

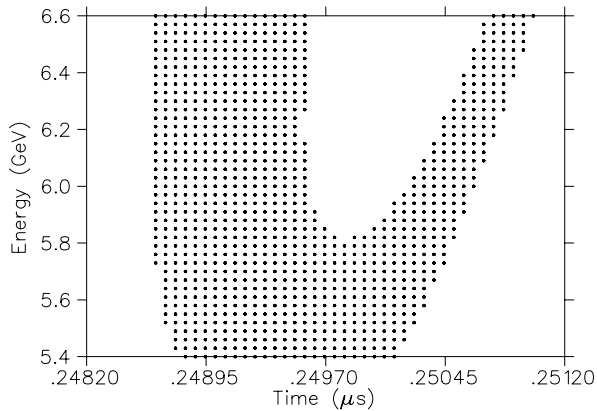


Figure 21: $\pm 10\%$ band from Input Acceptance

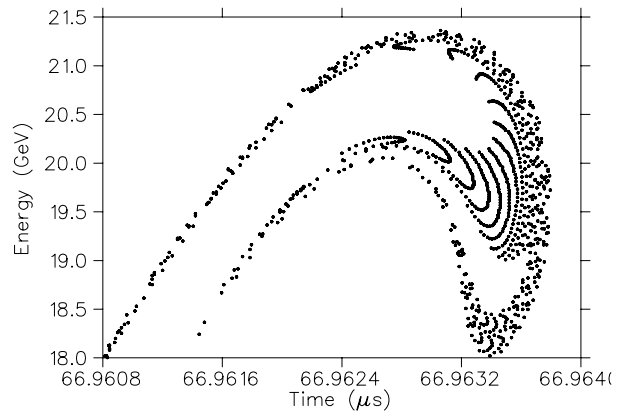


Figure 22: Maps to the Output Emittance, Case #33. Single harmonic, 30% over-voltage.

8 Other than 200 MHz

The phase slips accumulate half as quickly when the RF is halved, and so one anticipates that 100 MHz acceleration will be less compromised by using a larger number of turns. See cases 26,27,28,29,31. We have considered only the use of a single frequency and “best phases”, and no use of 2nd harmonic. The input admittance rises almost linearly from 3.0 to 3.7 eV.s as the number of turns is reduced from nine (case 29) to five (case 34).

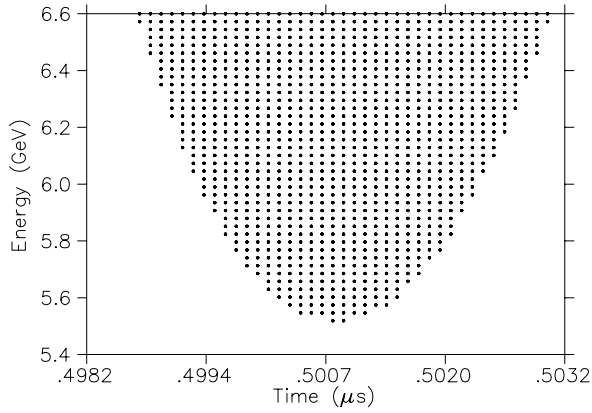


Figure 23: $\pm 10\%$ band from Input Acceptance

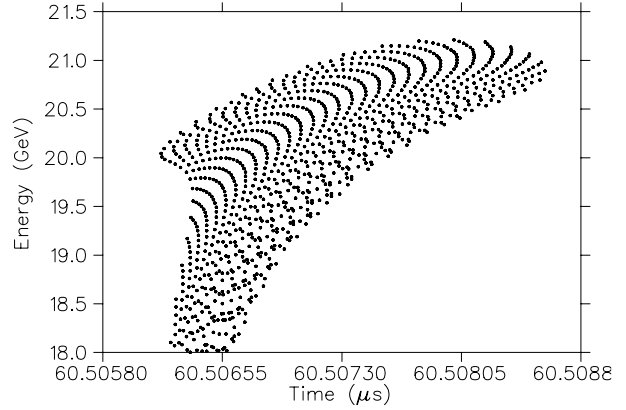


Figure 24: Maps to the Output Emittance, Case #29. 100 MHz, 9 turns.

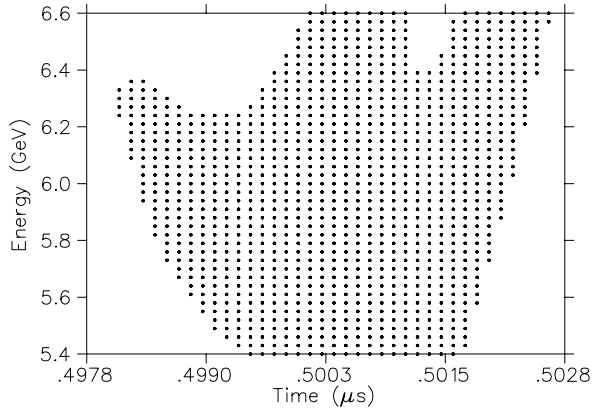


Figure 25: $\pm 10\%$ band from Input Acceptance

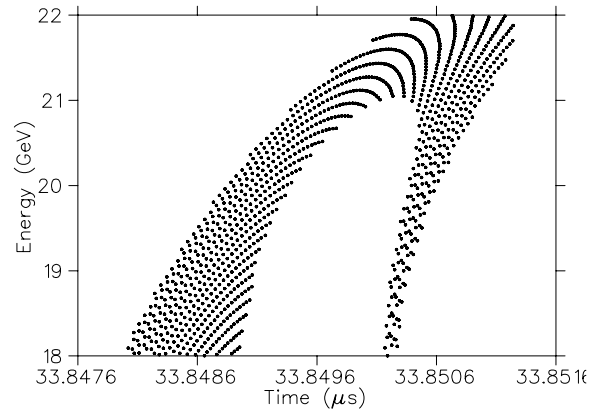


Figure 26: Maps to the Output Emittance, Case #34. 100 MHz, 5 turns.

Due to the extreme non-linear transport in case 34, the useful acceptance is much less than the advertized admittance of 3.7 eV.s. Increasing the number of turns to seven (case 27) or eight (case 28) reduces this effect (of non-linearity) quite substantially while maintaining useful admittances of 3.6 and 3.2 eV.s, respectively.

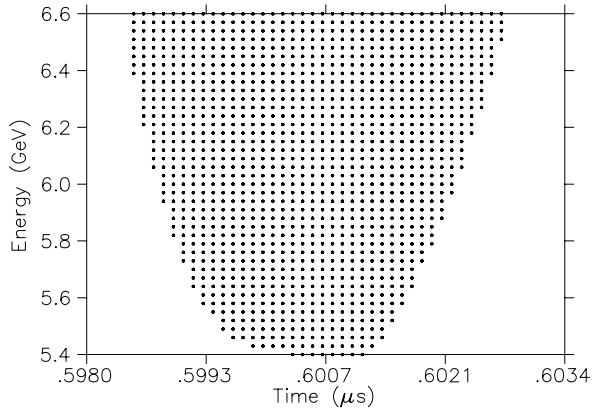


Figure 27: $\pm 10\%$ band from Input Acceptance

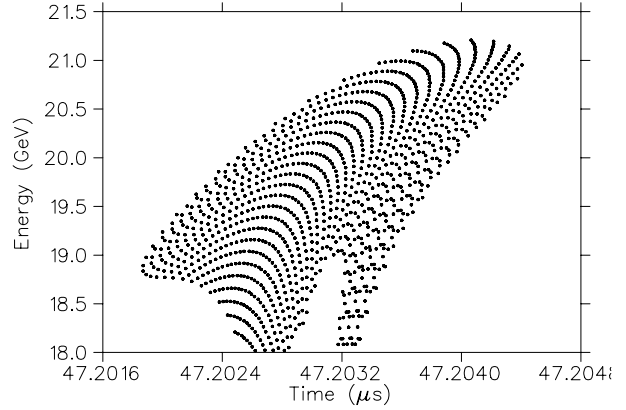


Figure 28: Maps to the Output Emittance, Case #27. 100 MHz, 7 turns.

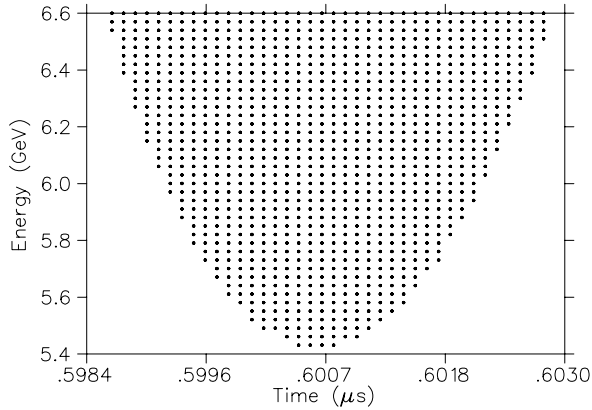


Figure 29: $\pm 10\%$ band from Input Acceptance

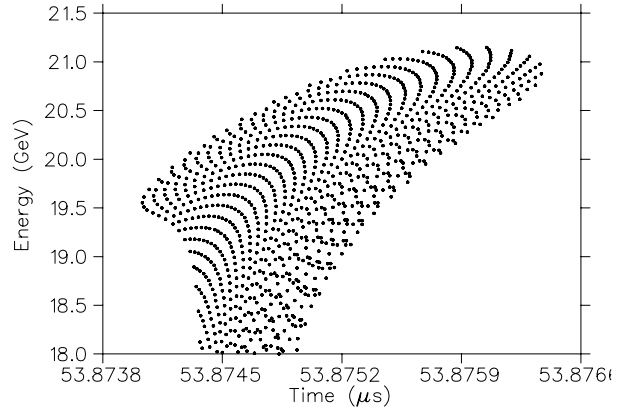


Figure 30: Maps to the Output Emittance, Case #28. 100 MHz, 8 turns.

8.1 10-turns

With minimal over-voltage, as an artefact of the optimizer, the transmission falls to zero for 10-turn acceleration. But notice how a greater over-voltage can restore transmission even for a ten-turn acceleration; compare case 26 (4% over voltage and zero transmission) with case 31 (30% over voltage and 1.8 eV.s acceptance).

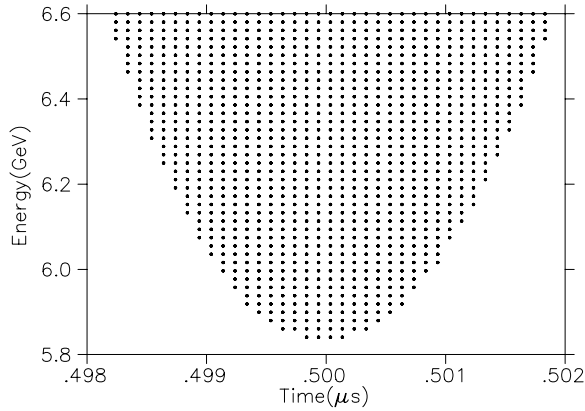


Figure 31: $\pm 10\%$ band from Input Acceptance

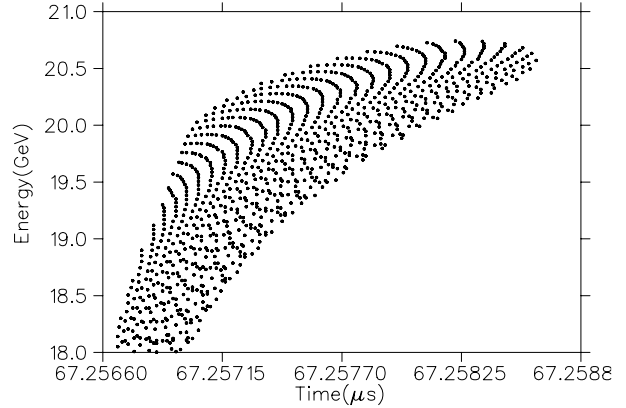


Figure 32: Maps to the Output Emittance, Case #31. 10 turns, 30% over voltage.

8.2 Conclusion

For acceleration with 100 MHz RF using a single frequency and fixed “best phases” (in the 2 km ring with 300 cells) the optimum number of turns appears to be seven or eight. However, if it is desirable to reduce the gradient, acceptable results can be achieved in 10 turns.

9 Other circumference

Just for fun we consider a machine with 1 km circumference but having a path-length-as-function-of-energy identical with the base 2 km machine. Since the beam spends less time in the machine, the phase slippage is smaller and consequently the longitudinal admittance is somewhat larger. See cases 3,4,1,2 which are all for 5-turn acceleration. Conclusions are very similar to those in section ?? . Dual harmonic is beneficial as is the use of a 20-30% over voltage.

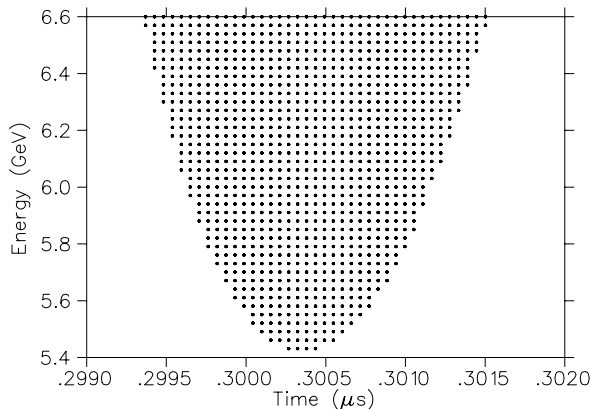


Figure 33: $\pm 10\%$ band from Input Acceptance

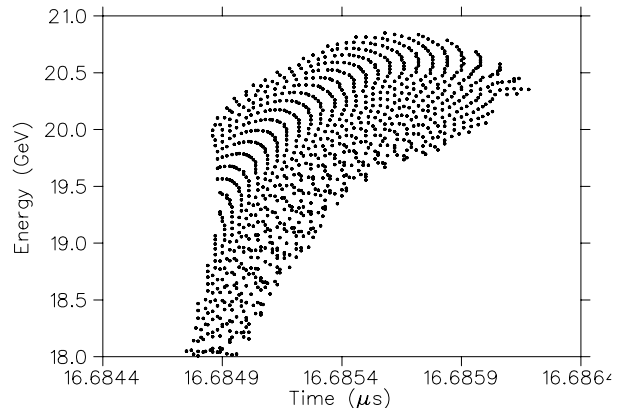


Figure 34: Maps to the Output Emittance, Case #1. Single harmonic and over-voltage.

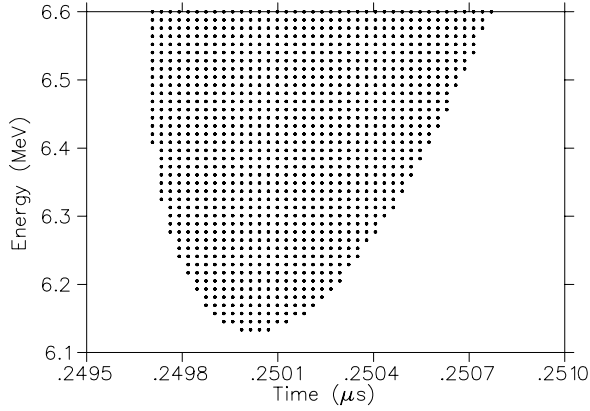


Figure 35: $\pm 10\%$ band from Input Acceptance

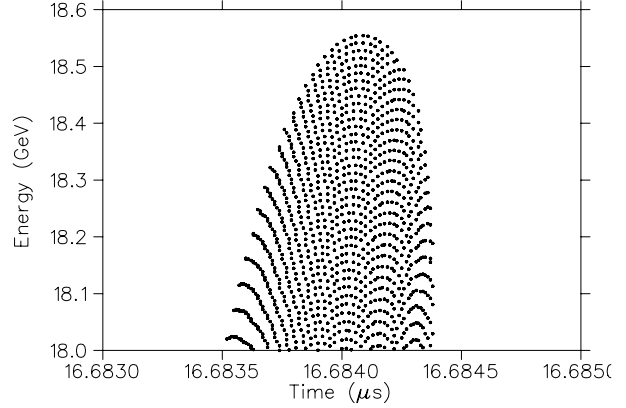


Figure 36: Maps to the Output Emittance, Case #4. Dual harmonic, no over-voltage.

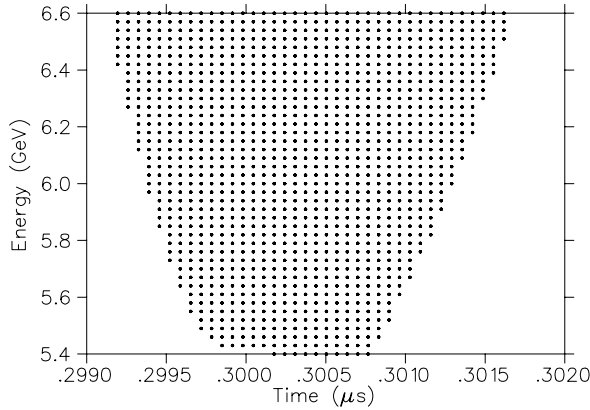


Figure 37: $\pm 10\%$ band from Input Acceptance

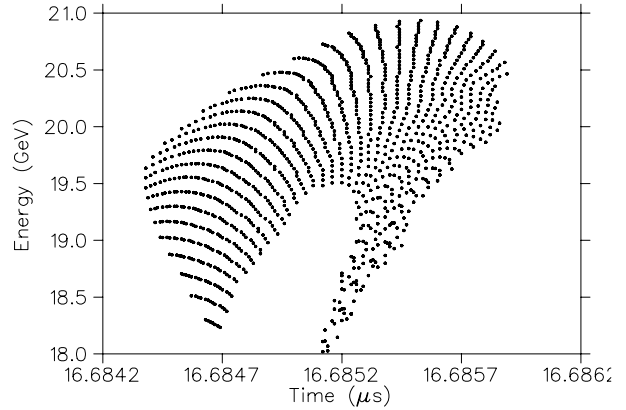


Figure 38: Maps to the Output Emittance, Case #2. Dual harmonic and over-voltage.

Compare figure 34 with 4, and figure 36 with 2, and figure 38 with 6, to appreciate the similarities.

10 Conclusion

Using a simple model we have studied the longitudinal dynamics of a muon beam in a 2 km circumference non-scaling FFAG, composed of roughly 300 equal cells, which operates between 6 and 20 GeV.

When 200 MHz RF is utilized, useful admittances can be achieved with acceleration in 5 or 6 (or less) turns using either ideal phases and nominal voltage or best phases and over voltage. In either case, transport is non-linear and the useful phase-space is compromised. In both cases, addition of 2nd harmonic roughly doubles the admittance but the non-linear effect is augmented. The non-linear effect of dual harmonic is most pronounced when ideal phases are used. If 9 or 10

turn acceleration is desired, then only the ideal phases scheme will provide successful acceleration; but the admittance is substantially reduced unless dual harmonic is employed.

For the case of 100 MHz RF, only the best phases and over voltage scenario was studied; and only for single harmonic operation. The optimal balance between quantity and quality of the output emittance is realized for 8-turn acceleration; but 7 or 9 turns also give acceptable results.

11 Cavity transient response in IQ form

Let ω be the carrier frequency. We write the cavity drive current $I(t)$ and the voltage response $V(t)$ in the IQ-form:

$$I(t) = I_a(t) \cos \omega t + I_b(t) \sin \omega t, \quad V(t) = V_a(t) \cos \omega t + V_b(t) \sin \omega t. \quad (8)$$

They are governed by the differential equation:

$$V'' + 2kV' + \omega_0^2 V = 2kRI, \quad (9)$$

where $2k = \omega_0/Q$, ω_0 is the resonance frequency and primes ($'$) denote time derivatives. We substitute the IQ forms and assume that V'' is small compared with $\omega^2 V$ (i.e. changes per cycle are small). For brevity let $\omega_0^2 = \omega^2 + \Delta$. We compare coefficients of $\cos \omega t$ and $\sin \omega t$ to obtain, respectively, the coupled equations

$$-2kR\omega I_b + 2k\omega V_b + \Delta \times V_a - 2kRI'_a + 2\omega V'_b + 2kV'_a = 0 \quad (10)$$

$$+2kR\omega I_a - 2k\omega V_a + \Delta \times V_b - 2kRI'_b - 2\omega V'_a + 2kV'_b = 0. \quad (11)$$

Let us define:

$$z_1 \equiv \frac{k(\Delta + 2\omega^2)}{2(k^2 + \omega^2)}, \quad z_2 \equiv \frac{\omega(\Delta - 2k^2)}{2(k^2 + \omega^2)}, \quad z_0 \equiv \frac{kR}{(k^2 + \omega^2)}. \quad (12)$$

Then the solution may be written

$$V_a = z_0 e^{-z_1 t} \left\{ \cos z_2 t \int_{-\infty}^t e^{z_1 s} [-F_1(s) \sin z_2 s + F_2(s) \cos z_2 s] ds \right. \\ \left. + \sin z_2 t \int_{-\infty}^t e^{z_1 s} [+F_1(s) \cos z_2 s + F_2(s) \sin z_2 s] ds \right\} \quad (13)$$

$$V_b = z_0 e^{-z_1 t} \left\{ \cos z_2 t \int_{-\infty}^t e^{z_1 s} [+F_1(s) \cos z_2 s + F_2(s) \sin z_2 s] ds \right. \\ \left. - \sin z_2 t \int_{-\infty}^t e^{z_1 s} [-F_1(s) \sin z_2 s + F_2(s) \cos z_2 s] ds \right\} \quad (14)$$

$$F_1 = -k\omega I_a + \omega^2 I_b + \omega I'_a + kI'_b \quad (15)$$

$$F_2 = +k\omega I_b + \omega^2 I_a - \omega I'_b + kI'_a. \quad (16)$$

Let us suppose that I_a and I_b are step functions rising from zero at T_a, T_b respectively, to the constant values I_a, I_b . Let Θ denote the Heaviside or unit-step function. Then the response becomes:

$$\begin{bmatrix} V_a \\ V_b \end{bmatrix} = z_3 \begin{bmatrix} C_1 & -C_2 \\ C_2 & C_1 \end{bmatrix} \begin{bmatrix} \cos z_2(t - T_a) & \sin z_2(t - T_b) \\ -\sin z_2(t - T_a) & \cos z_2(t - T_b) \end{bmatrix} \begin{bmatrix} I_a \Theta(t - T_a) e^{z_1(T_a - t)} \\ I_b \Theta(t - T_b) e^{z_1(T_b - t)} \end{bmatrix}. \quad (17)$$

Evidently, the transfer function is the matrix product of a coupling matrix and a rotation matrix. The coefficients of the coupling matrix are as follows.

$$C_1 = \frac{k(\Delta^2 - 4\omega^4)}{\omega 4(k^2 + \omega^2)} \rightarrow \frac{-k\omega^3}{k^2 + \omega^2} \rightarrow -k\omega \quad (18)$$

$$C_2 = \frac{\Delta^2 + 4(k\omega)^2}{4(k^2 + \omega^2)} + \frac{1}{2}\Delta \rightarrow \frac{(k\omega)^2}{k^2 + \omega^2} \rightarrow 0 \quad (19)$$

$$z_3 = R \frac{4k\omega}{\Delta^2 + 4(k\omega)^2} \rightarrow R \frac{1}{k\omega} \quad (20)$$

Here we have taken the limits first $\Delta \rightarrow 0$ and second $k \rightarrow 0$. In the same limits, one finds $z_1 \rightarrow k$, $z_2 \rightarrow -k^2/\omega$ and $z_0 \rightarrow Rk/\omega^2$.

In the limit $T_a, T_b \rightarrow -\infty$ one obtains the d.c. response:

$$V_a = R(+I_b\Delta + 2I_a k\omega)2k\omega/[\Delta^2 + 4(k\omega)^2] \quad (21)$$

$$V_b = R(-I_a\Delta + 2I_b k\omega)2k\omega/[\Delta^2 + 4(k\omega)^2]. \quad (22)$$

If the cavity is driven at its resonance frequency, $\Delta = 0$, then

$$V_a = I_a R \quad \text{and} \quad V_b = I_b R. \quad (23)$$

Because this is a linear system, one may invoke the principle of superposition to find the response to a series of step changes in the drive currents I_a, I_b .